25 GHz Operation of Silicon Optical Modulator with Projection MOS Structure

Junichi Fujikata[1], Jun Ushida[1], Yu Ming-Bin[2], Zhu ShiYang[2], Ding Liang[2], Patrick Lo Guo-Qiang[2], Dim-Lee Kwong[2] and Takahiro Nakamura[1]

[1] *NEC Corp., Nano Electronics Res. Labs., Tsukuba, Ibaraki 305-8501, Japan*

[2] *Institute of Microelectronics, A*STAR (Agency for Science, Technology and Research), 11 Science Park Road, Science Park-II, Singapore 117685*

j-fujikata@cj.jp.nec.com

Abstract:
We report a high-speed and compact silicon optical modulator based on the free carrier plasma dispersion in a silicon rib waveguide with a MOS (metal-oxide-semiconductor) junction structure. To achieve high-speed and high-efficiency performance, an improved structure of a very small rib waveguide including a projection MOS junction was studied. We demonstrated high speed of 25 GHz operation in case of 120-200 μm phase-shift length and high optical modulation efficiency of 0.5-0.67 Vcm for $V_{\pi}L$ by using a projection MOS junction structure. According to the carrier-density simulation, higher operation bandwidth up to 40 GHz can be realized.
©2010 Optical Society of America
OCIS codes: (250.7360) Waveguide modulators; (060.4080) Modulation; (203.7370) Waveguides;

1. Introduction

Silicon photonics has recently become a subject of intense interest because it offers an opportunity for low cost optoelectronic solutions for applications ranging from telecommunications down to chip-to-chip interconnects. In the past few years, there have been significant advances in pushing device performance of CMOS-compatible silicon blocks needed for developing silicon integrated photonic circuits. Fast silicon optical modulators (Si modulators) [1]-[3], SiGe photo-detectors [4], and hybrid silicon lasers [5] have been demonstrated. In order to satisfy the bandwidth and power requirements of next generation communication networks and future high performance computing applications, it would be desirable to realize significantly faster and very efficient Si modulators.

In this paper, we report the improved structure of a Si modulator with a projection MOS (metal-oxide-semiconductor) structure.

2. Device structure and fabrication

2-1 Device structure design

Figure 1 shows cross-sectional schematics of Si modulators in this study. We studied two types of Si modulators with (a) a flat MOS and (b) a projection MOS junction structures. A projection MOS junction structure is expected to enhance the free carrier plasma dispersion effect by improvement in overlapping between an optical field and a carrier modulation region. A rib waveguide structure includes the MOS junction, in which a slab layer of 300 nm-thick SOI (silicon-on-insulator) was boron-doped at the doping level of 0.5-5 x $10^{18}/cm^3$ and a phosphorous-doped poly-Si layer was stacked after growth of the 5 nm-thick gate-oxide layer. The poly-Si layer on the gate-oxide layer was patterned into 0.6 μm-width. The boron-doped slab layer was adjacent to highly-boron-doped regions to form a metal contact and a 100 nm-thick phosphorous-doped poly-Si layer was overlaid on the first poly-Si layer.

Figure 2 shows a cross-sectional optical field contour map for the rib waveguide. We designed it to maximize the overlapping between the optical field and the carrier modulation region by using a compact rib waveguide with highly-efficient optical confinement.

Figure 3 shows time dependence of integrated carrier density around the overlapping region for comparison between MOS and PN junction structures with the same rib waveguide, in case of DC bias which is initially raised from 0 V to +1 V or -1 V in 10 ps and maintained subsequently. In case of PN junction, carrier injection contributes to much larger carrier density change, but saturation time is much larger and is about 2 ns due to carrier recombination lifetime. So, operation with a negative bias should be applied for high-speed operation. On the other hand, in case of MOS junction, both carrier accumulation and depletion modes can be operated around 20 ps by choosing carrier density more than 1 x $10^{18}/cm^3$ in active layers.

Figure 4 shows time dependence of integrated carrier density for a flat and a projection MOS junction structures. By using a projection MOS junction structure, about 2-4 times larger carrier density modulation can be realized, even though a junction capacitance increases by 1.2-1.5 times. Therefore, a projection MOS

junction has potential of higher improvement in optical phase modulation efficiency. According to the simulation, increase of carrier density can achieve high-speed up to 40 GHz and more efficiency.

2-2 Device fabrication

Figure 5 shows (a) a picture and (b) a XTEM image of the fabricated Si modulator with a projection MOS structure. The Si modulator consists of an asymmetric Mach-Zehnder interferometer (MZI) structure with a built-in arm length difference of 20 μm to characterize the phase efficiency [2]. It starts from a boron-doped SOI wafer and patterned into a projection structure and a waveguide pattern. After 5 nm-thick gate-oxide of SiO_2 layer growth, an amorphous Si layer was deposited and annealed to form a poly-Si layer. After ion implantation process, an upper-clad of SiO_2 layer was deposited by PE-CVD and planarized by CMP, and an upper poly-Si layer was deposited on the rib waveguide as an electrode layer. Doping densities of SOI and poly-Si layers were changed from $5 \times 10^{17}/cm^3$ to $5 \times 10^{18}/cm^3$.

3. Device characterization

Figure 6(a) shows a DC response of the Si modulator with 120 μm phase shift length of a projection MOS junction. An asymmetric MZI structure produces an interference spectrum of 28.7 nm FSR (free spectral range) and 30 dB extinction ratio. By applying the DC bias of 2 V to one arm, an optical phase shift of about 1 nm occurred and 5-10 dB extinction ratio was obtained at a tuned wavelength. Figure of merit of $V_\pi L$ for this Si modulator was estimated to be 0.5-0.67 Vcm, which is about 8 times smaller than that of PN junction type [2]. Therefore, optical modulation efficiency for accumulation mode of the MOS junction is very high, compared with that for depletion mode of PN junctions. Insertion optical loss was 7.5 dB for the Si modulator with 120-200 μm phase shift length, including optical coupling loss of about 5 dB between an optical fiber and a Si channel waveguide for input and output. The waveguide loss of a modulator arm is about 7 dB/mm, which mainly originates from optical loss of the poly-Si waveguide and the high-doping poly-Si layer of an upper electrode. The Si modulator with a projection MOS junction showed a little more modulation efficiency than that for a flat MOS junction at present, because the waveguide loss of a modulator arm by the poly-Si waveguide surface roughness decreased the modulation efficiency. Therefore, much more modulation efficiency would be expected by improvement of poly-Si waveguide loss.

Figure 6 shows 12.5 GHz RF responses of the Si modulator in case of 2^{31}-1 PRBS patterns with (b) 2.5 V_{pp} and (c) 3.5 V_{pp}. Figure 6(d) shows a 25 GHz RF response in case of a 3.5 V_{pp} data signal sequence of 1and 0 bits. We obtained 3-6 dB extinction ratio only for 120 μm phase-shift length at 12.5 GHz. Both Si modulators of compact rib waveguides with a flat and a projection MOS junction structures showed very high-speed operation with very short phase-shift length, and these Si modulators would contribute to the highly-integrated silicon photonic circuits for the future networks and high performance computing.

4. Conclusions

We studied a high-speed and compact Si modulator based on the free carrier plasma dispersion in a compact Si rib waveguide with a MOS junction structure. To achieve high-speed and high-efficiency performance, an improved structure of a very small rib waveguide with a projection MOS junction was applied. We demonstrated high speed of 25 GHz operation in case of 120-200 μm phase-shift length and high modulation efficiency of 0.5-0.67 Vcm for $V_\pi L$ by using a projection MOS junction structure. According to the carrier-density simulation, higher operation bandwidth up to 40 GHz will be realized, by optimizing a MOS junction structure and carrier density.

Acknowledgements

The authors would like to thank Dr. S. Tahara for his advice and encouragement. The authors also thank Dr. A. Toda, Mr. M. Saitoh, Dr. T. Kato, Mr. M. Ishizaka, Dr. M. Nakada, Mr. T. Shimizu, and Mr. M. Noguchi for their discussions and technical assistances.

References

[1] A. Liu, R. Jones, L. Liao, d. Samara-Rubio, D. Rubin, O. Cohen, R. Nicolaescu, and M. Paniccia, “A high-speed silicon optical modulator based on a metal-oxide-semiconductor capacitor,” Nature 427, 615-618 (2004).

[2] A. Liu, L. Liao, D. Rubin, H. Nguyen, B. Ciftcioglu, Y. Chetrit, N. Izhaky, and M. Paniccia, “High-speed optical modulation based on carrier depletion in a silicon wavegide,” Opt. Express 15, 660-668 (2007).

[3] W. M. J. Green, M. J. Rooks, L. Sekaric, and Y. A. Vlasov, “Ultra-compact, low RF power, 10Gb/s silicon Mach-Zehnder modulator,” Opt. Express 15, 17106-17113 (2007).

[4] T. Yin, R. Cohen, M. M. Morse1, G. Sarid, Y. Chetrit, D. Rubin, and M. J. Paniccia, “31GHz Ge *n-i-p* waveguide photodetectors onSilicon-on-Insulator substrate,” Opt. Express 15, 13965-13971 (2007).

[5] A. W. Fang, H. Park, O. Cohen, R. Jones, M. Paniccia, J. E. Bowers, “Electrically pumped hybrid AlGaInAs-silicon evanescent laser,” Opt. Express 14, 9203-9210 (2006).

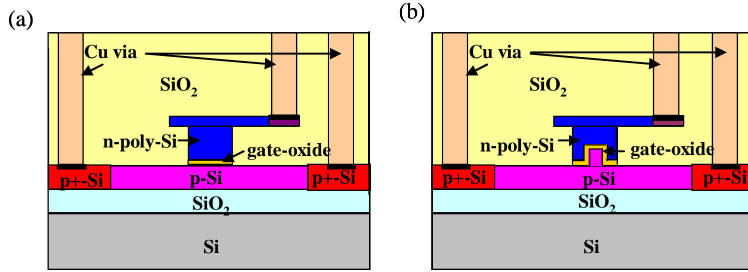

Fig. 1 Cross-sectional schematics of Si modulators with (a) flat MOS and (b) projection MOS junctions.

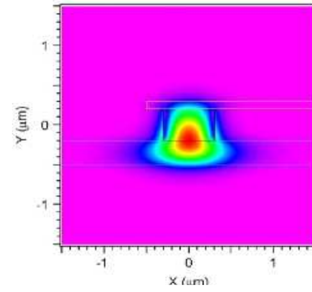

Fig. 2 Cross-sectional optical field contour map for the rib waveguide.

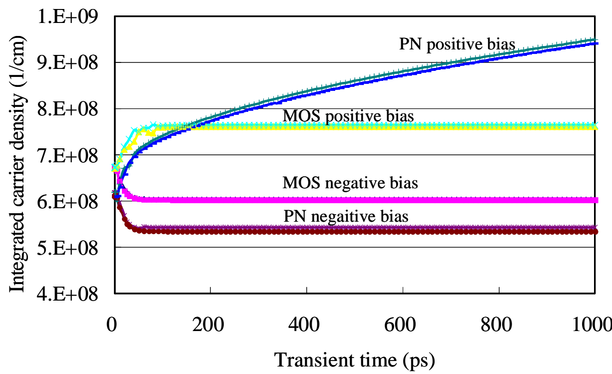

Fig. 3 Time dependence of integrated carrier density around the overlapping region for comparison between MOS and PN junction structures.

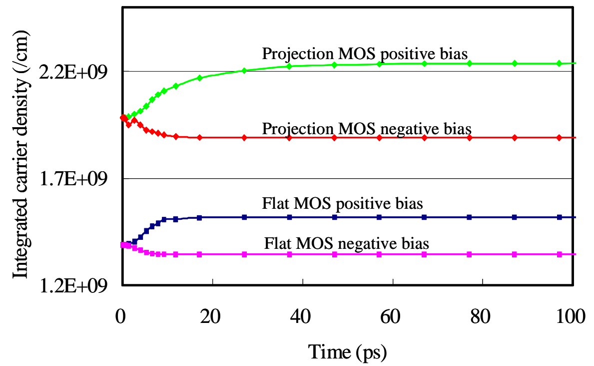

Fig. 4 Time dependence of integrated carrier density for flat and projection MOS junction structures.

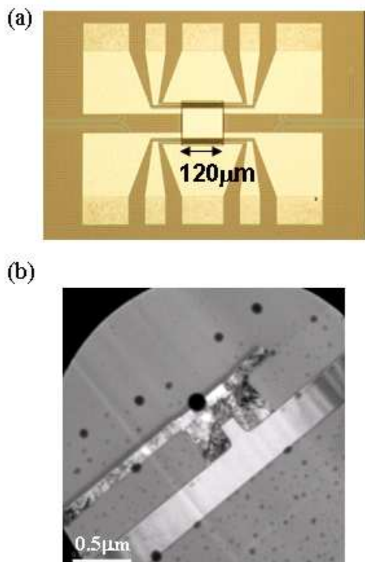

Fig. 5 (a) Picture and (b) XTEM image of the fabricated Si modulator with the projection MOS junction.

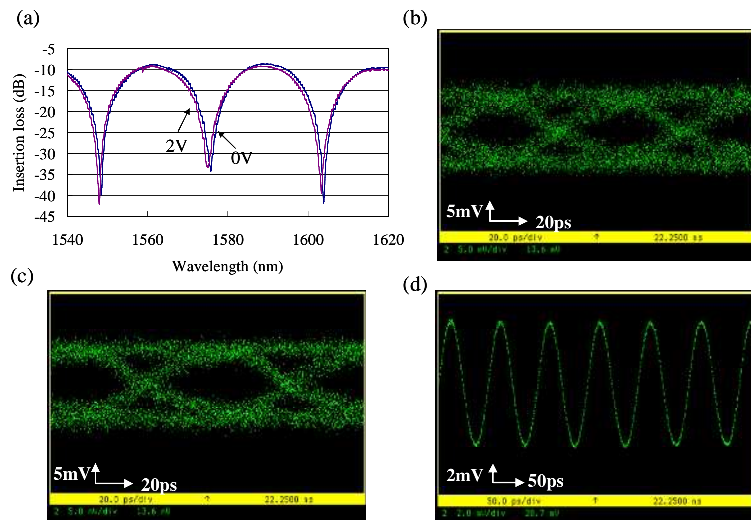

Fig. 6 (a) DC response of a Si modulator with 120μm phase shift. 12.5 GHz RF responses in case of 2^{31}-1 PRBS patterns with (b) 2.5 V_{pp} and (c) 3.5 V_{pp}. (d) 25 GHz RF response in case of a 3.5 V_{pp} data signal sequence of 1and 0 bits.